Published in final edited form as:
Cancer Immunol Immunother. 2013 April ; 62(4): 665–675. doi:10.1007/s00262-012-1372-8.

Enhancement of the Anti-Melanoma Response of Hu14.18K322A by αCD40+ CpG

Kory L. Alderson[1], **Mitchell Luangrath**[1], **Megan M. Elsenheimer**[1], **Stephen D. Gillies**[2], **Fariba Navid**[3], **Alexander L. Rakhmilevich**[1,4], and **Paul M. Sondel**[1,4,5]

[1] Department of Human Oncology, University of Wisconsin-Madison, Madison WI

[2]Provenance Biopharmaceuticals Corp., Burlington MA

[3]Department of Oncology, St. Jude Children's Research Hospital, Memphis, TN

[4]Paul Carbone Comprehensive Cancer Center, University of Wisconsin-Madison, Madison WI

[5]Department of Pediatrics, University of Wisconsin-Madison, Madison WI

Abstract

Targeted monoclonal antibodies (mAb) can be used therapeutically for tumors with identifiable antigens such as disialoganglioside GD2, expressed on neuroblastoma and melanoma tumors. Anti-GD2 mAbs (αGD2) can provide clinical benefit in patients with neuroblastoma. An important mechanism of mAb therapy is Antibody Dependent Cellular Cytotoxicity (ADCC). Combinatorial therapeutic strategies can dramatically increase the anti-tumor response elicited by mAbs. We combined a novel αGD2 mAb, hu14.18K322A, with an immunostimulatory regimen of agonist CD40 mAb and class B CpG-ODN 1826 (CpG). Combination immunotherapy was more effective than the single therapeutic components in a syngeneic model of GD2-expressing B16 melanoma with minimal tumor burden. NK cell depletion in B6 mice showed NK cells were required for the anti-tumor effect; however, anti-tumor responses were also observed in tumor-bearing SCID/beige mice. Thus NK cell cytotoxicity did not appear to be essential. Peritoneal macrophages from anti-CD40+CpG treated mice inhibited tumor cells *in vitro* in an hu14.18K322A antibody-dependent manner. These data highlight the importance of myeloid cells as potential effectors in immunotherapy regimens utilizing tumor-specific mAb and suggest further studies are needed to investigate the therapeutic potential of activated myeloid cells and their interaction with NK cells.

Keywords

GD2; melanoma; Antibody-dependent Cellular Cytotoxicity (ADCC); CD40; Macrophage; NK cell

Introduction

The most common immunotherapy for the treatment of cancer is monoclonal antibody (mAb) therapy. The anti-tumor effects of tumor-targeted mAbs generally occur through the activation of complement and/or antibody-dependent cellular cytotoxicity (ADCC) and/or antibody-dependent phagocytosis (ADCP) [1]. To maximize anti-tumor responses elicited by mAbs, much research has focused on immune activation alongside mAb administration.

Paul M Sondel, University of Wisconsin-Madison, 1111 Highland Ave- WIMR 4156, Madison, WI 53705.

We report here on a combinatorial approach, with a unique mAb, hu14.18K322A, combined with anti-CD40 mAb (αCD40) and CpG, both potent stimuli of innate immune cells.

Hu14.18K322A is a humanized mAb that targets ganglioside D2 (GD2), a glycoshpingolipid overexpressed by tumors of neuroectodermal origin, such as melanoma and neuroblastoma [2, 3]. Hu14.18K322A was specifically designed to minimize toxicities associated with anti-GD2 (αGD2) therapy. Due to limited expression of GD2 on healthy peripheral nervous tissue, the major dose limiting toxicity associated with anti-GD2 therapy is allodynia and is dependent on complement activation [4]. One unique property of hu14.18K322A is a targeted mutation at amino acid 322 that replaces a lysine with an alanine. This specific mutation reduces antibody-mediated complement activation. Additionally, hu14.18K322A is produced in the rat hybridoma cell line YB2/0 that has low fucosyltransferase activity. Monoclonal antibodies with such altered side chains on the Fc portion are more potent inducers of ADCC [5, 6]. Combined, these unique features of hu14.18K322A are designed to reduce complement-related toxicities, while maximizing effector responses by cells mediating ADCC.

Previous reports from our laboratory have used αCD40 either alone, or in combination with a class B CpG nucleotide in several tumor therapy models [7, 8]. αCD40 is a member of the TNF receptor superfamily and is found on many cells such as myeloid cells, endothelial cells, and platelets, among other cells. Agonist antibodies to CD40 (αCD40) initiate potent activation of cells expressing CD40, including dendritic cells and macrophages. CpG 1826 is a class B CpG-ODN that is recognized by TLR9. αCD40+ CPG immunotherapy produces anti-tumor responses through the activation of innate immune effector cells such as NK cells and macrophages [9, 10]. Since many of the effector cell populations activated by αCD40+ CpG are capable of mediating ADCC or ADCP, we tested the ability of αCD40+ CpG to augment tumor-targeted mAb responses.

The studies presented in this report sought to maximize the anti-tumor effect of hu14.18K322A in a model of murine melanoma by co-administration of a CD40 agonist and TLR9 stimulus, CpG. In a model of minimal disease, we found a significant increase in the anti-tumor activity of hu14.18K322A when it was combined with αCD40+ CpG. Therapeutic efficacy was independent of T cells and re-challenge studies indicated that immunological memory was not induced. We found a potential role for both NK cells and macrophages in the hu14.18K322A-mediated response. Overall, our data presented here demonstrated a clear enhancement of hu14.18K322A-dependent anti-tumor activity when mAb is combined with activation of innate effector cells using αCD40 + CpG.

Materials and Methods

Mice and tumor cell lines

Six to 10 week old C57BL/6 or SCID/beige mice (Taconic Farms) were housed and cared for in accordance with the Guide for Care and Use of Laboratory Animals and under an animal protocol approved by the Animal Care and Use Committee. B78D14 tumor cells are a B16F10 melanoma derivative cell line transfected with the gene coding β-1,4-N-acetylgalactosaminyltransferase resulting in the constitutive expression of GD2 on the cell surface [11]. Cells were grown in RPMI 1640 complete cell culture medium supplemented with 10% heat inactivated FCS (Sigma-Aldrich), 2mM L-glutamine, 100U/mL penicillin and streptomycin at 37 °C and 5% CO_2. Cells were cultured two passages prior to injection with 400μg/mL Geneticin Neomycin and 50μg/mL Hygromycin B for selection of cells expressing GD2. C57BL/6 mice were injected subcutaneously on the left abdomen with the indicated tumor cell number in 0.1mL. Subcutaneous tumor growth was measured at

indicated days after tumor implantation and tumor volume was calculated using the formula [volume mm^3 = (length) × ($width^2$) × (0.52)].

Therapy regimen (αCD40+ CpG + hu14.18K322A)

For αCD40+ CpG therapy, 0.25mg (0.2mL) of αCD40 [clone FGK45.5 (a gift from Dr. F. Melchers, Basel Institute for Immunology, Basel Switzerland) rat anti-mouse agonist antibody was purified and confirmed as previously described [10]] was injected intraperitoneally (i.p.) on indicated days. 0.05mg (0.2 mL) of endotoxin-free, phosphorothioate-modified, CpG 1826, 5'TCCATGACGTTCCTGACGTT-3' (TriLink Biotechnology, San Diego, CA) was injected i.p. in 0.2mL, three days after αCD40 priming. Hu14.18K322A (provided by St. Jude Children's Research Hospital and the Children's GMP, LLC, Memphis, TN.) is a genetically engineered form of the hu14.18 humanized anti-GD2 monoclonal antibody that has been mutated to prevent complement activation and grown in Y2 cells to limit fucosylation and enhance ADCC [4]. Hu14.18K322A was administered intravenously (25μg/dose in 0.2mL) for five consecutive days beginning the day after the first αCD40 injection.

For depletion studies, 0.1mg αNK1.1 mAb, clone PK136 (ATCC) was injected i.p. in 0.2mL starting two-days prior to the first dose of αCD40 and repeated every three days for the first week of therapy while hu14.18K322A mAb was administered.

In vitro assay of macrophage activity

Peritoneal exudate was collected by peritoneal lavage one day after one round of αCD40+ CpG. Peritoneal exudate cells (PEC) were added to a 96-well round bottom plate at 0.1mL of cell suspension at 10^6 cells/mL and serially diluted in the plate. Cells were then incubated for 1.5–2hr to allow for plastic adherence of macrophages, after which time non-adherent cells were removed by gently pipetting. 10^4 tumor cells were added per well with10μg/mL of hu14.18K322A. The assay was incubated overnight at 37°C and 5% CO_2. After overnight incubation, 1μCi of ^{3}H-thymidine was added per well and incubated an additional 6–10Hrs. Total cells were harvested from the wells and onto a fiberglass filter using a Packard cell harvester, and relative beta counts were determined using a Packard Matrix 9600 direct beta counter (Packard instruments). Conditions were assayed in triplicate with 2–4 mice per experiment. The average count of each condition was graphed as a single point and the averages of individual mice were graphed as replicates.

Depletion of macrophages in vivo

For some studies, phagocytic cells were depleted in vivo by injection of clodronate liposomes as previously described [12]. Clodronate was a gift from Roche Diagnostics GmbH, Mannheim, Germany.

Flow Cytometry

To test for hu14.18K322A-labeling of B78D14 tumor cells, 1μg of hu14.18K322A mAb used in therapeutic studies was incubated with 10^5 tumor cells at 4°C for 30min, excess was washed off, and 1μg of polyclonal PE-anti-human IgG (eBioscience, San Diego, CA) was secondarily used to detect bound hu14.18K322A. To determine macrophage loss after plate adherence, all of the cells that were removed from the plate or 10^5 PEC not adhered to plastic, were labeled with 0.5μg of each antibody, PE-Cy5 αF4/80 (clone BMB, eBioscience, San Diego CA) and Pacific Blue-αCD11b (Clone M1/70, Biolegend, San Diego, CA) for 30min at 4°C. All flow cytometry was acquired on a BD LSRII (BD, San Jose, CA) and analyzed using FlowJo software (Treestar, Ashland, OR).

Statistics

Kaplan-Meier survival curves were generated and analyzed in Prism graphical software (Graphpad, La Jolla, CA); differences in survival were determined by applying a log-rank test. Tumor growth data were analyzed using a two-way ANOVA, and differences in F4/80+ cells in the peritoneal fluid pre- and post-plastic adherence were determined by applying a Student's t-test. Data are presented as mean ± SD and considered significantly different when P values are below 0.05.

Results

αCD40+CpG priming followed by hu14.18K322A can cure melanoma-bearing mice in a minimal disease setting

Our initial hypothesis was that the priming of innate immune effector cells with αCD40+ CpG would increase the anti-tumor effect of hu14.18K322A. Previous reports from our laboratory have shown that αCD40+ CpG immunotherapy activates both NK cells and macrophages [9, 8, 10]. Furthermore, both NK cells and macrophages are effector cells capable of mediating ADCC against antibody coated tumor cells [13–16]. To address this hypothesis, we used a B16 melanoma tumor cell line that expresses GD2, B78D14, and is recognized by hu14.18K322A mAb (Figure 1A).

To evaluate a combinatorial effect of αCD40+ CpG and hu14.18K322A, we treated C57BL/6 mice bearing subcutaneous B78D14 tumors with combination immunotherapy or with each therapeutic component, i.e. hu14.18K322A alone or αCD40+ CpG. In some experiments, combination therapy started at different times after tumor injection; however, once therapy was initiated, a standard timing regimen was followed (Figure 1B). For our initial experiments, we began treatment of mice early, before mice had palpable tumors, 5 days after injection of tumor cells, and evaluated therapeutic efficacy by monitoring subcutaneous tumor growth and overall survival. Tumors in mice treated with combination immunotherapy, consisting of anti-CD40+ CpG and hu14.18K322A, grew considerably slower than tumors in mice that were treated with either component of the regimen (Figure 1C). Many mice that received combination immunotherapy did not develop detectable tumors, leading to a significant increase in overall survival (Figure 1D). These results indicate that anti-CD40+ CpG co-administration enhances the antitumor effectiveness of tumor-targeted mAb, hu14.18K322A, in a setting of minimal disease burden.

Because we observed complete and prolonged anti-tumor responses in mice with very small (non-palpable) tumors, we evaluated efficacy of combination immunotherapy against larger, more established tumors. We implanted mice with two initial doses of tumor cells, 0.5×10^6 and 2×10^6, and started therapy at 3 different time points, day 5, 18 or 28 after tumor implantation (Figure 2A). The results of these studies indicated that tumor burden in this model affects the level of response to this form of combination immunotherapy. When mice were implanted with a smaller number of tumor cells, tumor growth inhibition and the likelihood of survival inversely correlated with the start of therapy (Figure 2 B and C). When mice were implanted with a larger number of tumor cells, only the earliest treatment regimen provided any detectible anti-tumor effect (Figure 2 D and E). These data indicate that this combination immunotherapy in this model has maximum efficacy in situations of minimal disease.

To address a potential role of immunological memory in mice surviving long-term, we compared tumor growth in mice rendered tumor-free by this combined immunotherapy regimen and in aged matched control mice. Long-term tumor-free mice were defined as mice that had been challenged with tumor and received combined immunotherapy (as in Figures 1 and 2) and survived with undetectable tumor for at least 100 days after the last

tumor-bearing mouse had been sacrificed. We did not observe a difference in tumor growth between long-term tumor-free mice and aged matched controls challenged with tumor for the first time (Figure 2F). From these experiments, we concluded that combination immunotherapy was not inducing detectible immunological memory; this suggested that the antitumor effect was likely being mediated by innate immune effector cells.

Anti-tumor effect of a combination of anti-CD40+CpG and hu14.18K322A in SCID/Beige mice

To test whether T and B cell adaptive immune responses as well as NK cell-mediated ADCC are needed for this *in vivo* immunotherapeutic effect, we treated B78-bearing SCID/beige mice; these mice are deficient in T and B cells and have a lysosomal mutation that impairs the cytolytic function of their NK cells [17, 18]. They were implanted with tumor and treated with αCD40+ CpG and hu14.18K322A. Most mature NK cells constitutively express Fc-receptors (FcRs) and are powerful mediators of ADCC against antibody-opsonized targets [19], but NK cells of SCID/beige mice are unable to mediate ADCC. Previous studies from our laboratory have shown antitumor effects *in vivo* from αCD40+ CpG in SCID/beige mice bearing B16F10 melanoma tumors; depletion studies suggest that at least some component of this antitumor effect results from macrophage-mediated tumor destruction [7]. We implanted SCID/beige mice with 0.5×10^6 B78D14 melanoma tumor cells and followed tumor growth after treatment with combination immunotherapy or with either therapeutic component. Similar to our observations in normal C57BL/6 mice (Figure 1C), tumor growth was significantly slowed in SCID/beige mice when they were treated with combination immunotherapy (Figure 3A). Unlike wild-type (WT) C57BL/6 mice, we saw only a small separation between the anti-tumor activity of αCD40+ CpG alone and the combination immunotherapy (Figure 3A). The greater difference in the tumor growth inhibition by the combined therapy (vs. αCD40+ CpG alone) in the WT mice (Fig. 2 B) than in SCID/beige mice (Figure 3A) likely represents the partial contribution of NK-cell mediated lysis in WT mice in our therapy model. While αCD40+ CpG treated mice had slower initial tumor growth than control mice (Figure 3A), all of these mice developed tumor and their survival time was not increased compared to control mice (Figure 3B). However, some SCID/beige mice treated with combination immunotherapy remained tumor-free and this translated into a significant increase in their survival time (Figure 3B). These data suggest that combination mAb-based immunotherapy retains some anti-tumor function in the absence of T cells, B cells and NK cell-mediated lysis.

To further dissect the role of NK cells in the functional efficacy of combination immunotherapy, we depleted NK cells from tumor-bearing B57BL/6 mice with anti-NK1.1 mAb and treated them with combination immunotherapy (Figure 4A). Interestingly, while earlier studies suggested that mechanisms other than NK-cell mediated lysis could play a role in the anti-tumor responses, depletion studies suggested that the presence of NK cells was necessary. Depletion of NK cells with αNK1.1 mAb prior to, and during combination immunotherapy virtually abrogated the anti-tumor effect (Figure 4A and B). Anti-tumor efficacy was also abrogated in mice depleted of phagocytic cells with chlodronate-containing liposomes [12]; however, since mice treated with control PBS-containing liposomes showed a slight but significant reduction in therapeutic benefit, these data were inconclusive (data not shown).

Activation of myeloid cells after anti-CD40+ CpG in vivo

After observing anti-tumor activity in the absence of NK cell-mediated lysis, we used an *in vitro* system to evaluate the role of macrophages against hu14.18K322A-opsonized tumor cells. Macrophages and other myeloid cells are capable effectors against mAb-opsonized tumor cells [20–23]. Furthermore, αCD40+ CpG can activate macrophages *in vivo* to have

tumoricidal activity [7]. We used plastic adherence to isolate macrophages, then co-cultured the adherent macrophages with tumor cells overnight (Figure 5A). Flow cytometric analysis of the cell suspension before and after plastic adherence suggested that the vast majority of the macrophages in the PEC population were retained by adherence on the plate (Figure 5B - D), however we did not see a significant difference in the expression level of the Fc receptors CD16 or CD32 (Data not shown).

To test macrophage activity, we used macrophages from control or αCD40+ CpG primed mice in a coculture assay against tumor cells +/− hu14.18K322A (Figure 6A). With this system, we observed potent anti-tumor activity by αCD40+ CpG primed macrophages in an antibody dependent manner. These observations were consistent using peritoneal cells from normal C57BL/6 mice (Figure 6B), CB.17 SCID mice (Figure 6C), and SCID/beige mice (Figure 6D). Slight but significant increases in tumor cell lysis were observed in an 18-hr 51Cr-release assay, suggesting that adherent peritoneal cells from αCD40+ CpG primed mice had increased cytotoxic capabilities (data not shown). These data suggest that αCD40+ CpG primed macrophages can inhibit tumor cell proliferation in an antibody-dependent manner and may participate in the combinatorial anti-tumor effect of anti-CD40+ CpG and hu14.18K322A *in vivo*.

Discussion

In this manuscript, we showed that the anti-tumor effectiveness of hu14.18K322A *in vivo* is enhanced by αCD40+ CpG therapy. The benefit of combining hu14.18K322A with αCD40+ CpG was particularly apparent in mice with small tumors. Notably, therapeutic efficacy depended more on tumor amount than time of establishment (Figure 2), indicating this regimen may be effective in minimal residual disease. Combined therapy (with hu14.18K322A added to αCD40+ CpG), was effective at eradicating small tumors and led to long-term survival in some animals; this was not seen in the experiments when mice received only hu14.18K322A or only αCD40+ CpG. Long-term survival occurred in immunocompetent mice without inducing immunological memory, and also could be induced by combined therapy in mice lacking T cells.

Secondary induction of adaptive immunity after monoclonal antibody-based therapy has been observed in various tumor models [24–26], but the mechanism and the dominant effector cell population depends on the tumor type. Recently, Abes et al observed the induction of a persistent, T-cell dependent, anti-tumor response elicited by αCD20 mAb, CAT-13 [24]. However, T cell involvement is likely tumor dependent as our group has previously shown that immunocytokine therapy with anti-EpCAM-IL-2 can induce a T cell response against tumor with high MHC class I expression, but not against low MHC class I variants of the same tumor [27]. In the latter case with poor MHC expression, NK cells are the dominant effector cell that responds to immunocytokine and persistent T cell immunity is not achieved [27]. In this manuscript, we are using B78D14 tumor cells, a subclone of B16-F10. B16-F10 is well documented to have low expression of MHC class I, which may be one reason we did not observe a T cell response in this model.

We investigated the potential role of NK cells and macrophages, as both are capable of mediating ADCC. We have previously reported that αCD40 can activate both NK cells and macrophages in tumor bearing mice [28, 10]. Our data presented here indicate that NK cells are required for therapeutic efficacy *in vivo*(Figure 4B); however, studies using SCID/beige mice suggested that lytic function of NK cells might not be a requirement (Figure 3) *in vivo*. Recently, a model of allogeneic cell rejection was used to demonstrate that macrophage effector functions cannot be well deciphered in vivo unless NK cell function is impaired [29]. Previous studies from our laboratory [9] and others [30] have shown that interferon-γ

(IFNγ) is required for macrophage activation in certain mouse models of tumor immunotherapy. NK cells are the primary source of IFNγ after in vivo administration of CpG + antibody-coated tumor cells [31]. Furthermore, co-administration of interleukin-12 alongside Trastuzumab therapy produces greater antitumor responses and is dependent on NK cell production of IFNγ[32]. Both anti-CD40 [10] and CpG 1826 [33] promote secretion of IFNγ when administered independently. Therefore, while it may be difficult to separate the independent contributions of macrophages and NK cells *in vivo*, NK cell production of IFNγ in SCID/beige mice that would be absent in NK cell depleted mice may explain the difference in results between these two settings (Figure 3 and Figure 4).

Enhancement of ADCC by CpG-activation of effector cells was initially shown in the late 1990's in a mouse model of B cell lymphoma [34]. Much of this was assumed to be the direct activation NK cells, which has been described for both human and mouse NK cells [35, 31]. Subsequently, two classes of CpG-containing oligoneucleotides, class-A and -B, were described to activate different effector populations involved in ADCC [36]. In vivo depletion studies have been used to show that while CpG-A-enhanced ADCC requires only NK cells, CpG-B-enhanced ADCC is mediated by both NK cell and granulocytes [36]. CpG therapy was combined with rituximab in a phase II trial in patients with follicular lymphoma, in which responses were similar to those previously reported for rituximab alone [37]. However, the patients in the combination trial had all undergone prior rituximab treatment, and therefore comparison of the two reported response rates may be unfair [37]. The route of CpG administration may affect its ability to enhance ADCC. Intratumoral CpG rather than systemic CpG was shown to be better at increasing the anti-tumor activity of an αCD20 antibody [38]. In our model system, we have observed that priming with αCD40 increases the expression of TLR9 by macrophages peaking at three days after αCD40. Therefore, we used this information to devise our treatment regimen. We believe that in addition to activating macrophages and other cells of the innate immune system, αCD40 is sensitizing cells to TLR9 activation resulting in an augmented response to CpG.

Studies depleting macrophages *in vivo* with clodronate liposomes [12] were inconclusive in our hands; while the anti-tumor effect of the combined therapy was substantially reduced by treatment with the clodronate liposomes, treatment of tumor bearing mice with control, PBS-containing, liposomes also slightly but significantly reduced the anti-tumor effect of therapy. However, a recent publication by Tsai and colleagues suggested that phagocytosis of gold particles larger than 4nm in size reduced the cellular response to TLR9 [39]. Tsai et al. concluded that the effect was due to a gold-specific interference of high mobility groupbox 1 that regulates TLR9 signaling. As they did not compare gold nanoparticles to a non-gold control, they could not conclusively say if the inhibition of TLR9 responses was restricted to gold particles, or possibly a function of phagocytosis of large particles [39]. Since we observed a decrease in therapeutic efficacy when mice were treated with PBS-liposomes, we were concerned that the ingestion of liposome particles may have decreased the functional response to TLR9 stimulation. Therefore, we used an in vitro system to evaluate macrophage-mediated anti-tumor activity.

αCD40 -primed macrophages can act as effector cells against numerous mouse and human tumors [7, 40– 42]. αCD40 activated human macrophages mediate anti-tumor responses to human pancreatic cancer [43]. Few reports have evaluated CD40 and/or CpG activation of macrophages for increasing antibody responses. The data presented here demonstrate at least a partial role for αCD40+ CPG primed macrophages in the response to tumor-targeted hu14.18K322A.

Using a co-culture system, we found that enriched αCD40+ CpG primed macrophages could inhibit tumor cell proliferation in an antibody-dependent manner (Figure 6). These in vitro

data suggest that macrophages are involved in the anti-tumor response. Clinical data from our laboratory have recently suggested that myeloid cells may play a role in the therapeutic effect of mAb in neuroblastoma patients [20, 44, 45]. In a small phase II study of hu14.18-IL2 immunocytokine, we observed a clear association between the expression of a high affinity Fc receptor on myeloid cells (CD32) and clinical response [20, 45]. Furthermore, we participated in recently demonstrating that αGD2 mAb ch14.18, when combined with GM-CSF and interleukin-2 (IL2) is better than the standard of care for high-risk neuroblastoma patients [44]. Although not compared directly, ch14.18 + GMCSF + IL2 appeared to have a bigger impact on survival than ch14.18-IL2 mAb alone, without GMCSF [45, 44, 46]. While more data are needed, these two studies may suggest an important role for myeloid cells in the response to αGD2 mAbs in patients with neuroblastoma.

Acknowledgments

This work was supported by National Institutes of Health Grants CA032685, CA87025, CA166105, CA14520, GM067386, Department of Defense grant W81XWH-08-1-0559 and grants from the Midwest Athletes for Childhood Cancer Fund, the Crawdaddy Foundation and The Evan Dunbar Foundation.

References

1. Koehn TA, Trimble LL, Alderson KL, Erbe AK, McDowell KA, Grzywacz B, Hank JA, Sondel PM. Increasing the clinical efficacy of NK and antibody-mediated cancer immunotherapy: potential predictors of successful clinical outcome based on observations in high-risk neuroblastoma. Front Pharmacol. 2012; 3:91. [PubMed: 22623917]
2. Alderson KL, Sondel PM. Clinical cancer therapy by NK cells via antibody-dependent cell-mediated cytotoxicity. J Biomed Biotechnol. 2011; 2011:379123. [PubMed: 21660134]
3. Yamane BH, Hank JA, Albertini MR, Sondel PM. The development of antibody-IL-2 based immunotherapy with hu14.18-IL2 (EMD-273063) in melanoma and neuroblastoma. Expert Opin Investig Drugs. 2009; 18(7):991–1000.
4. Sorkin LS, Otto M, Baldwin WM 3rd, Vail E, Gillies SD, Handgretinger R, Barfield RC, Ming Yu H, Yu AL. Anti-GD(2) with an FC point mutation reduces complement fixation and decreases antibody-induced allodynia. Pain. 2010; 149(1):135–142. [PubMed: 20171010]
5. Shinkawa T, Nakamura K, Yamane N, Shoji-Hosaka E, Kanda Y, Sakurada M, Uchida K, Anazawa H, Satoh M, Yamasaki M, Hanai N, Shitara K. The absence of fucose but not the presence of galactose or bisecting N-acetylglucosamine of human IgG1 complex-type oligosaccharides shows the critical role of enhancing antibody-dependent cellular cytotoxicity. J Biol Chem. 2003; 278(5): 3466–3473. [PubMed: 12427744]
6. Zeng Y, Fest S, Kunert R, Katinger H, Pistoia V, Michon J, Lewis G, Ladenstein R, Lode HN. Anti-neuroblastoma effect of ch14.18 antibody produced in CHO cells is mediated by NK-cells in mice. Mol Immunol. 2005; 42(11):1311–1319. [PubMed: 15950727]
7. Buhtoiarov IN, Lum HD, Berke G, Sondel PM, Rakhmilevich AL. Synergistic activation of macrophages via CD40 and TLR9 results in T cell independent antitumor effects. J Immunol. 2006; 176(1):309–318. [PubMed: 16365423]
8. Buhtoiarov IN, Sondel PM, Eickhoff JC, Rakhmilevich AL. Macrophages are essential for antitumour effects against weakly immunogenic murine tumours induced by class B CpG-oligodeoxynucleotides. Immunology. 2007; 120(3):412–423. [PubMed: 17163960]
9. Buhtoiarov IN, Lum H, Berke G, Paulnock DM, Sondel PM, Rakhmilevich AL. CD40 ligation activates murine macrophages via an IFN-gamma-dependent mechanism resulting in tumor cell destruction in vitro. J Immunol. 2005; 174(10):6013–6022. [PubMed: 15879094]
10. Turner JG, Rakhmilevich AL, Burdelya L, Neal Z, Imboden M, Sondel PM, Yu H. Anti-CD40 antibody induces antitumor and antimetastatic effects: the role of NK cells. J Immunol. 2001; 166(1):89–94. [PubMed: 11123280]
11. Straten PT, Guldberg P, Seremet T, Reisfeld RA, Zeuthen J, Becker JC. Activation of preexisting T cell clones by targeted interleukin 2 therapy. Proc Natl Acad Sci U S A. 1998; 95(15):8785–8790. [PubMed: 9671756]

12. Van Rooijen N, Sanders A. Liposome mediated depletion of macrophages: mechanism of action, preparation of liposomes and applications. J Immunol Methods. 1994; 174(1–2):83–93. [PubMed: 8083541]

13. Dyall R, Vasovic LV, Clynes RA, Nikolic-Zugic J. Cellular requirements for the monoclonal antibody-mediated eradication of an established solid tumor. Eur J Immunol. 1999; 29(1):30–37. doi:10.1002/(SICI)1521-4141(199901)29:01<30::AID-IMMU30>3.0.CO;2-D [pii] 10.1002/(SICI)1521-4141(199901)29:01<30::AID-IMMU30>3.0.CO;2-D. [PubMed: 9933083]

14. Hank JA, Albertini MR, Schiller J, Sondel PM. Activation of multiple effector mechanisms to enhance tumor immunotherapy. J Immunother Emphasis Tumor Immunol. 1993; 14(4):329–335. [PubMed: 8280716]

15. Ralph P, Nakoinz I. Cooperation of IgG monoclonal antibodies in macrophage antibody-dependent cellular cytotoxicity (ADCC) to tumor targets. J Leukoc Biol. 1984; 35(1):131–139. [PubMed: 6584510]

16. Uchida J, Hamaguchi Y, Oliver JA, Ravetch JV, Poe JC, Haas KM, Tedder TF. The innate mononuclear phagocyte network depletes B lymphocytes through Fc receptor-dependent mechanisms during anti-CD20 antibody immunotherapy. J Exp Med. 2004; 199(12):1659–1669. [PubMed: 15210744]

17. Roder JC. The beige mutation in the mouse. I. A stem cell predetermined impairment in natural killer cell function. J Immunol. 1979; 123(5):2168–2173. [PubMed: 489978]

18. Roder JC, Lohmann-Matthes ML, Domzig W, Wigzell H. The beige mutation in the mouse. II. Selectivity of the natural killer (NK) cell defect. J Immunol. 1979; 123(5):2174–2181. [PubMed: 158612]

19. Yokoyama WM, Kim S, French AR. The dynamic life of natural killer cells. Annu Rev Immunol. 2004; 22:405–429. [PubMed: 15032583]

20. Delgado DC, Hank JA, Kolesar J, Lorentzen D, Gan J, Seo S, Kim K, Shusterman S, Gillies SD, Reisfeld RA, Yang R, Gadbaw B, DeSantes KB, London WB, Seeger RC, Maris JM, Sondel PM. Genotypes of NK cell KIR receptors, their ligands, and Fcgamma receptors in the response of neuroblastoma patients to Hu14.18-IL2 immunotherapy. Cancer Res. 2010; 70(23):9554–9561. [PubMed: 20935224]

21. Joshi T, Ganesan LP, Cheney C, Ostrowski MC, Muthusamy N, Byrd JC, Tridandapani S. The PtdIns 3-kinase/Akt pathway regulates macrophage-mediated ADCC against B cell lymphoma. PLoS One. 2009; 4(1):e4208. [PubMed: 19148288]

22. Leidi M, Gotti E, Bologna L, Miranda E, Rimoldi M, Sica A, Roncalli M, Palumbo GA, Introna M, Golay J. M2 macrophages phagocytose rituximab-opsonized leukemic targets more efficiently than m1 cells in vitro. J Immunol. 2009; 182(7):4415–4422. [PubMed: 19299742]

23. Oflazoglu E, Stone IJ, Brown L, Gordon KA, van Rooijen N, Jonas M, Law CL, Grewal IS, Gerber HP. Macrophages and Fc-receptor interactions contribute to the antitumour activities of the anti-CD40 antibody SGN-40. Br J Cancer. 2009; 100(1):113–117. [PubMed: 19066610]

24. Abes R, Gelize E, Fridman WH, Teillaud JL. Long-lasting antitumor protection by anti-CD20 antibody through cellular immune response. Blood. 2010; 116(6):926–934. [PubMed: 20439625]

25. Clynes R, Takechi Y, Moroi Y, Houghton A, Ravetch JV. Fc receptors are required in passive and active immunity to melanoma. Proc Natl Acad Sci U S A. 1998; 95(2):652–656. [PubMed: 9435247]

26. Fridman WH, Teillaud JL, Sautes-Fridman C, Pages F, Galon J, Zucman-Rossi J, Tartour E, Zitvogel L, Kroemer G. The ultimate goal of curative anti-cancer therapies: inducing an adaptive anti-tumor immune response. Front Immunol. 2011; 2:66. [PubMed: 22566855]

27. Imboden M, Murphy KR, Rakhmilevich AL, Neal ZC, Xiang R, Reisfeld RA, Gillies SD, Sondel PM. The level of MHC class I expression on murine adenocarcinoma can change the antitumor effector mechanism of immunocytokine therapy. Cancer Res. 2001; 61(4):1500–1507. [PubMed: 11245457]

28. Rakhmilevich AL, Baldeshwiler MJ, Van De Voort TJ, Felder MA, Yang RK, Kalogriopoulos NA, Koslov DS, Van Rooijen N, Sondel PM. Tumor-associated myeloid cells can be activated in vitro and in vivo to mediate antitumor effects. Cancer Immunol Immunother. 2012

29. Liu W, Xiao X, Demirci G, Madsen J, Li XC. Innate NK cells and macrophages recognize and reject allogeneic nonself in vivo via different mechanisms. J Immunol. 2012; 188(6):2703–2711. [PubMed: 22327074]
30. Saddawi-Konefka ROST, Vermi W, et al. Cancer immunoediting by the innate immune system in the absence of adaptive immunity. Journal of Immunology Meeting Abstract Supplement. 2012; 188(162.3)
31. Roda JM, Parihar R, Carson WE 3rd. CpG-containing oligodeoxynucleotides act through TLR9 to enhance the NK cell cytokine response to antibody-coated tumor cells. J Immunol. 2005; 175(3): 1619–1627. [PubMed: 16034101]
32. Jaime-Ramirez AC, Mundy-Bosse BL, Kondadasula S, Jones NB, Roda JM, Mani A, Parihar R, Karpa V, Papenfuss TL, LaPerle KM, Biller E, Lehman A, Chaudhury AR, Jarjoura D, Burry RW, Carson WE 3rd. IL-12 enhances the antitumor actions of trastuzumab via NK cell IFN-gamma production. J Immunol. 2011; 186(6):3401–3409. [PubMed: 21321106]
33. Xin L, Shelite TR, Gong B, Mendell NL, Soong L, Fang R, Walker DH. Systemic treatment with CpG-B after sublethal rickettsial infection induces mouse death through indoleamine 2,3-dioxygenase (IDO). PLoS One. 2012; 7(3):e34062. [PubMed: 22470514]
34. Wooldridge JE, Ballas Z, Krieg AM, Weiner GJ. Immunostimulatory oligodeoxynucleotides containing CpG motifs enhance the efficacy of monoclonal antibody therapy of lymphoma. Blood. 1997; 89(8):2994–2998. [PubMed: 9108420]
35. Ballas ZK, Rasmussen WL, Krieg AM. Induction of NK activity in murine and human cells by CpG motifs in oligodeoxynucleotides and bacterial DNA. J Immunol. 1996; 157(5):1840–1845. [PubMed: 8757300]
36. van Ojik HH, Bevaart L, Dahle CE, Bakker A, Jansen MJ, van Vugt MJ, van de Winkel JG, Weiner GJ. CpG-A and B oligodeoxynucleotides enhance the efficacy of antibody therapy by activating different effector cell populations. Cancer Res. 2003; 63(17):5595–5600. [PubMed: 14500400]
37. Friedberg JW, Kelly JL, Neuberg D, Peterson DR, Kutok JL, Salloum R, Brenn T, Fisher DC, Ronan E, Dalton V, Rich L, Marquis D, Sims P, Rothberg PG, Liesveld J, Fisher RI, Coffman R, Mosmann T, Freedman AS. Phase II study of a TLR-9 agonist (1018 ISS) with rituximab in patients with relapsed or refractory follicular lymphoma. Br J Haematol. 2009; 146(3):282–291. [PubMed: 19519691]
38. Betting DJ, Yamada RE, Kafi K, Said J, van Rooijen N, Timmerman JM. Intratumoral but not systemic delivery of CpG oligodeoxynucleotide augments the efficacy of anti-CD20 monoclonal antibody therapy against B cell lymphoma. J Immunother. 2009; 32(6):622–631. [PubMed: 19483647]
39. Tsai CY, Lu SL, Hu CW, Yeh CS, Lee GB, Lei HY. Size-dependent attenuation of TLR9 signaling by gold nanoparticles in macrophages. J Immunol. 2012; 188(1):68–76. [PubMed: 22156340]
40. Buhtoiarov IN, Rakhmilevich AL, Lanier LL, Ranheim EA, Sondel PM. Naive mouse macrophages become activated following recognition of L5178Y lymphoma cells via concurrent ligation of CD40, NKG2D, and CD18 molecules. J Immunol. 2009; 182(4):1940–1953. [PubMed: 19201847]
41. Lum HD, Buhtoiarov IN, Schmidt BE, Berke G, Paulnock DM, Sondel PM, Rakhmilevich AL. In vivo CD40 ligation can induce T-cell-independent antitumor effects that involve macrophages. J Leukoc Biol. 2006; 79(6):1181–1192. [PubMed: 16565324]
42. Rakhmilevich AL, Buhtoiarov IN, Malkovsky M, Sondel PM. CD40 ligation in vivo can induce T cell independent antitumor effects even against immunogenic tumors. Cancer Immunol Immunother. 2008; 57(8):1151–1160. [PubMed: 18214476]
43. Beatty GL, Chiorean EG, Fishman MP, Saboury B, Teitelbaum UR, Sun W, Huhn RD, Song W, Li D, Sharp LL, Torigian DA, O'Dwyer PJ, Vonderheide RH. CD40 agonists alter tumor stroma and show efficacy against pancreatic carcinoma in mice and humans. Science. 2011; 331(6024):1612–1616. [PubMed: 21436454]
44. Yu AL, Gilman AL, Ozkaynak MF, London WB, Kreissman SG, Chen HX, Smith M, Anderson B, Villablanca JG, Matthay KK, Shimada H, Grupp SA, Seeger R, Reynolds CP, Buxton A, Reisfeld RA, Gillies SD, Cohn SL, Maris JM, Sondel PM. Anti-GD2 antibody with GM-CSF,

interleukin-2, and isotretinoin for neuroblastoma. N Engl J Med. 2010; 363(14):1324–1334. [PubMed: 20879881]

45. Shusterman S, London WB, Gillies SD, Hank JA, Voss SD, Seeger RC, Reynolds CP, Kimball J, Albertini MR, Wagner B, Gan J, Eickhoff J, DeSantes KB, Cohn SL, Hecht T, Gadbaw B, Reisfeld RA, Maris JM, Sondel PM. Antitumor activity of hu14.18-IL2 in patients with relapsed/refractory neuroblastoma: a Children's Oncology Group (COG) phase II study. J Clin Oncol. 2010; 28(33):4969–4975. [PubMed: 20921469]
46. Simon T, Hero B, Faldum A, Handgretinger R, Schrappe M, Niethammer D, Berthold F. Consolidation treatment with chimeric anti-GD2-antibody ch14.18 in children older than 1 year with metastatic neuroblastoma. J Clin Oncol. 2004; 22(17):3549–3557. [PubMed: 15337804]

A

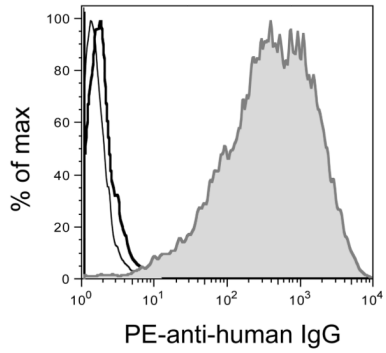

B

Treatment Regimen

Day 1	Day 2	Day 3	Day 4	Day 5	Day 6	Day 8	Day 11	
αCD40	K322A	K322A	K322A +CpG	K322A	K322A	αCD40	CpG	Tumor growth and survival

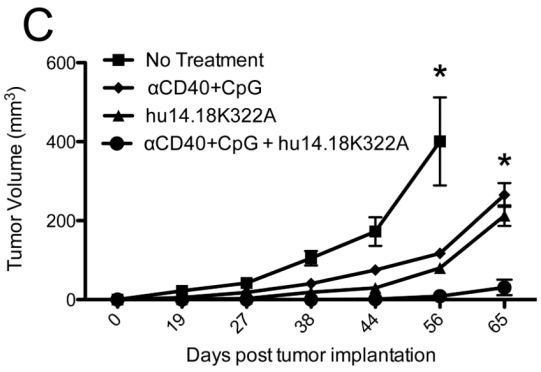

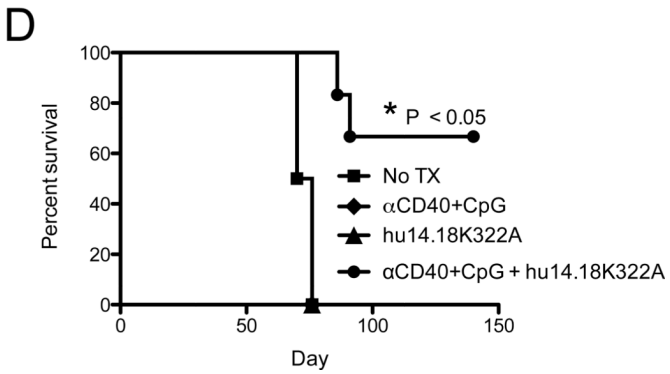

Figure 1. αCD40+ CpG Immunotherapy Enhances the Anti-tumor Response of hu14.18K322A

A) A flow cytometry histogram showing binding of hu14.18K322A to B78D14 tumor cells. The bold and thin lines represent isotype control and PE secondary only control, respectively. The shaded area is binding of hu14.18K322A. **B)** A schematic showing the regimen of αCD40+ CpG and hu14.18K322A. The regimen begins at varying times after tumor implantation, but follows a standard timing regimen once begun. The indicated day represents the day of therapy (where treatment begins on day1), not days after tumor implantation. **C and D)** C57BL/6 mice were implanted subcutaneously with 0.5×10^6 B78D14 tumor cells on day 0, and therapy was initiated 5 days after tumor cell implantation.

Tumor cell growth **(C)** and overall survival **(D)** were followed after cessation of immunotherapy (and plotted based on the days after tumor implantation). Tumor growth and survival analyses consist of 6–8 mice per group and are representative of at least three independent experiments. * $P < 0.05$ indicates a significant difference between the combination therapy (αCD40 + CpG + hu14.18K322A) group and all other groups on days 56 and 65 in (**C**), and for the comparison of the combination group survival curve to the other 3 in (**D**). In **(D)** the survival curves of the 3 groups other than the combination group are all superimposed on one another. Statistical analyses were completed using a two-way ANOVA (tumor growth), or a Log-rank test (survival).

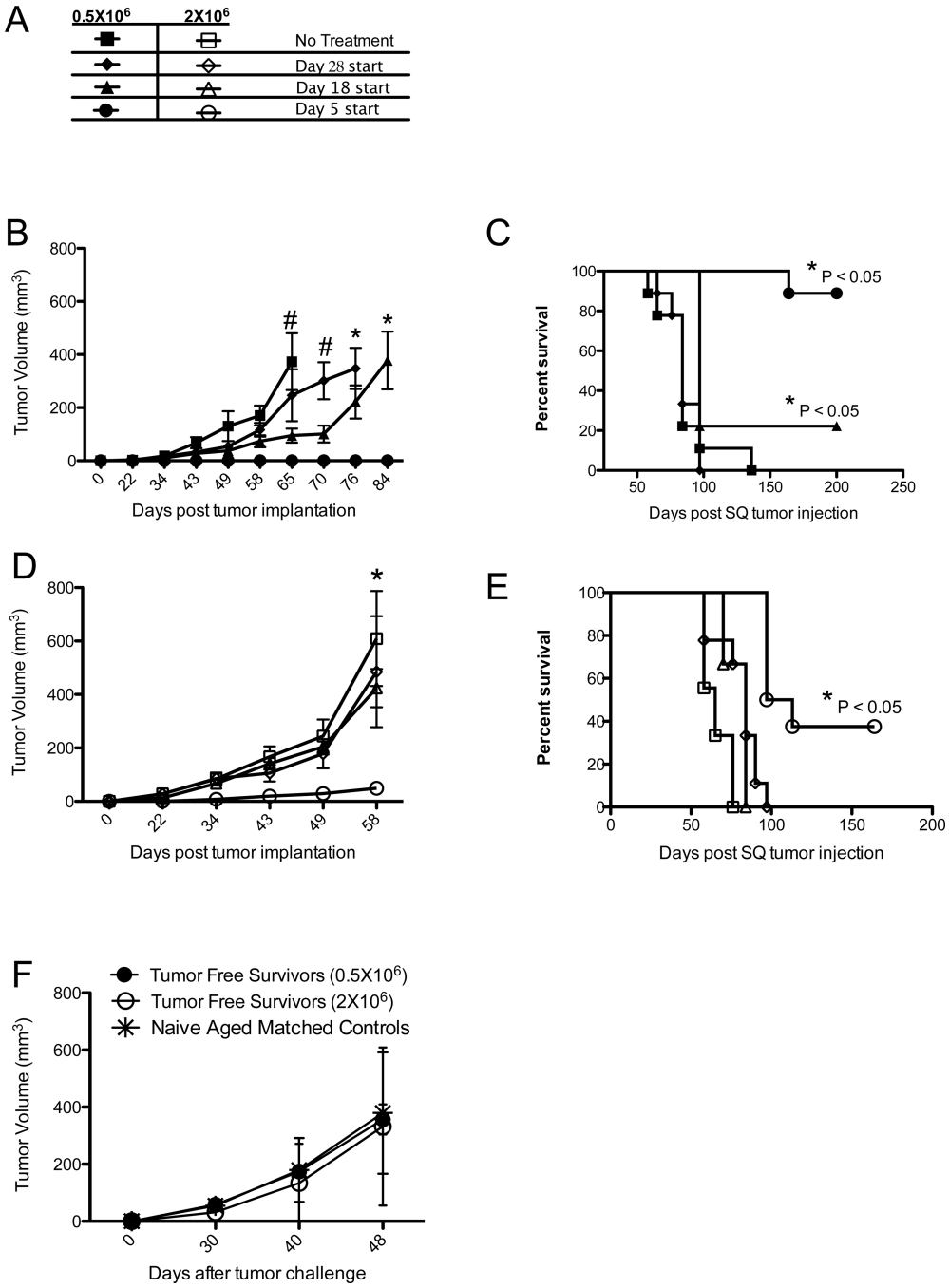

Figure 2. Combination Immunotherapy Results in Long-term Cure of Mice Without Inducing Immunological Memory

A) Provision of the key to symbols used in Figure 2B-E, showing the symbols corresponding to mice that were implanted with either 0.5×10^6 tumor cells (closed symbols, in **B** and **C**) or 2×10^6 tumor cells (open symbols, in **D** and **E**) and given combination therapy starting on days 5, 18 or 28 after tumor implantation. **B-E)** Mice implanted with varying tumor doses with varying immunotherapy start days as indicated in **(A)** were monitored for tumor growth (**B** and **D**) or survival (**C** and **E**). **F)** Mice living longer than 100 days without detectable tumor were re-challenged with 2×10^6 B78D14 subcutaneously (SQ) and tumor growth was compared to the growth of 2×10^6 B78D14 implanted subcutaneously in aged

matched control mice not previously implanted with tumor. In **(B)** and **(D)**, # = $P < 0.05$ for treatment starting on day 5 versus control and day 28 start, or * = $P < 0.05$ for treatment starting on day 5 versus all other groups, determined by two way ANOVA. Each graph consists of 4 or more mice per group and are representative of at least two independent experiments.

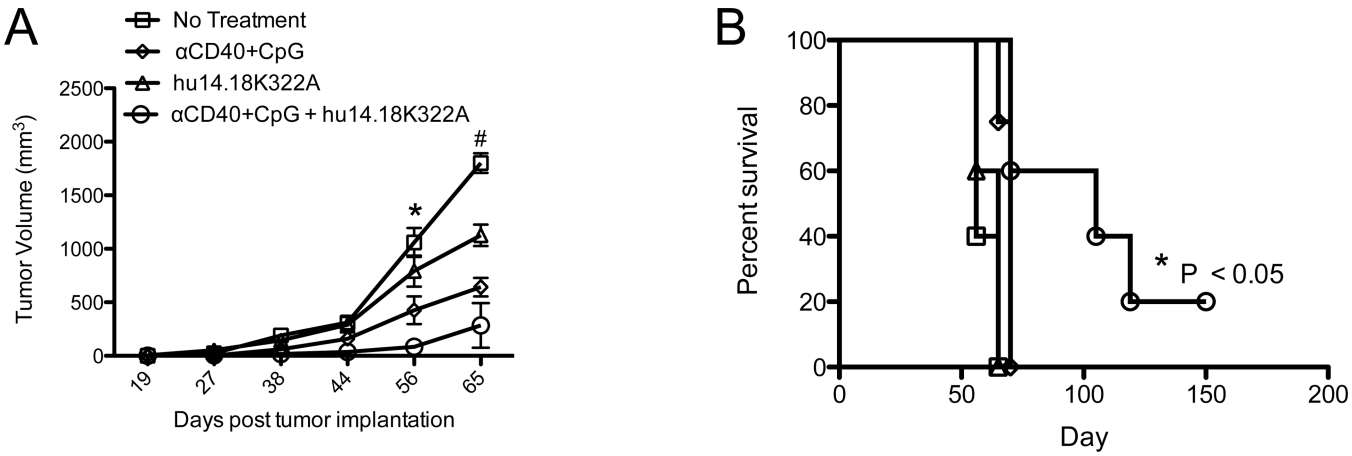

Figure 3. Combination Therapy Remains Effective in the Absence of Cell-Mediated Cytotoxicity

SCID/beige mice lacking T cells, B cells and having NK cells with minimal cytolytic activity were implanted with 0.5×10^6 B78D14 tumor cells on day 0 and combination or single immunotherapy was started on day 5. **A)** Tumor growth and **B)** survival were monitored over time. *P < 0.05 as determined by two-way ANOVA and compares combination immunotherapy to all other groups. #P < 0.05 by two-way ANOVA comparing combination group against control and hu14.18K322A alone. Graphs show groups of 4–8 mice per group and are representative of 2 independent experiments.

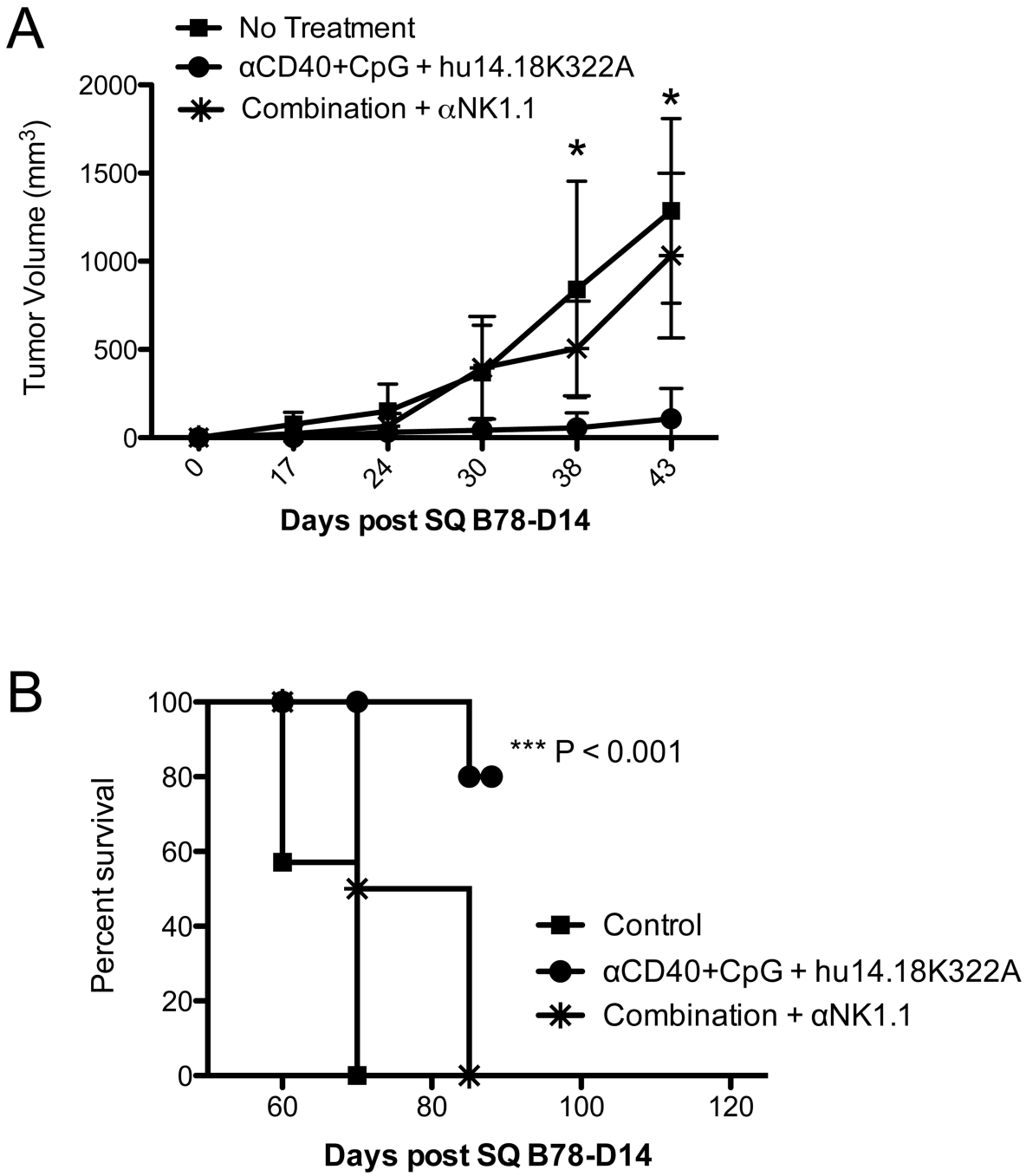

Figure 4. NK cells are required in vivo for the anti-tumor response to hu14.18K322A

B6 mice were implanted with 0.5×10^6 B78D14 tumor cells on day 0 and combination immunotherapy was begun on day 5. Natural killer cells were depleted by injection of αNK1.1 mAb on days −2, 3, and 8 of therapy. **A)** Tumor growth and **B)** survival were monitored over time. * $P < 0.05$ comparing combination therapy group with all other groups (control, combo+ depletion), and was determined by applying a two-way ANOVA. Graphs show groups consisting of 4–6 mice per group and are representative of 2 independent experiments.

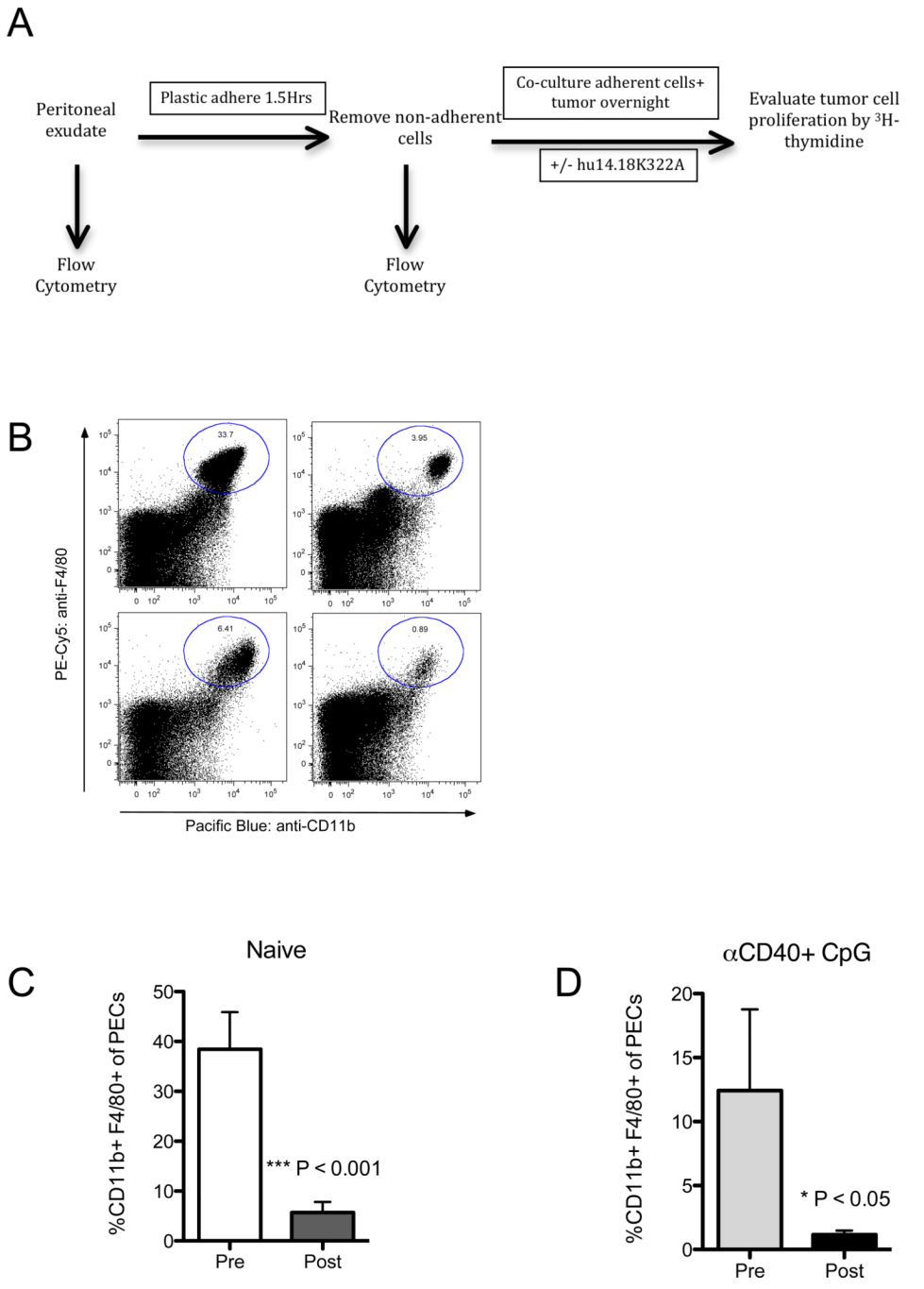

Figure 5. In vitro Assay of Macrophage Anti-tumor Activity

A) Assay schematic of *in vitro* system used to evaluate anti-tumor activity by macrophages. **B)** Representative flow cytometry dot plots of peritoneal exudate before the plastic adherence and the cells that were removed following the plastic adherence step of the *in vitro* assay; macrophages were defined as CD11b+ F4/80+. **C)** Bar graphs showing that macrophages were left on the plate by comparing the percentage of macrophages in the peritoneal fluid pre and post plastic adherence. Bar graphs are the combination of 4 mice per group and significant differences were determined by a student's t-test.

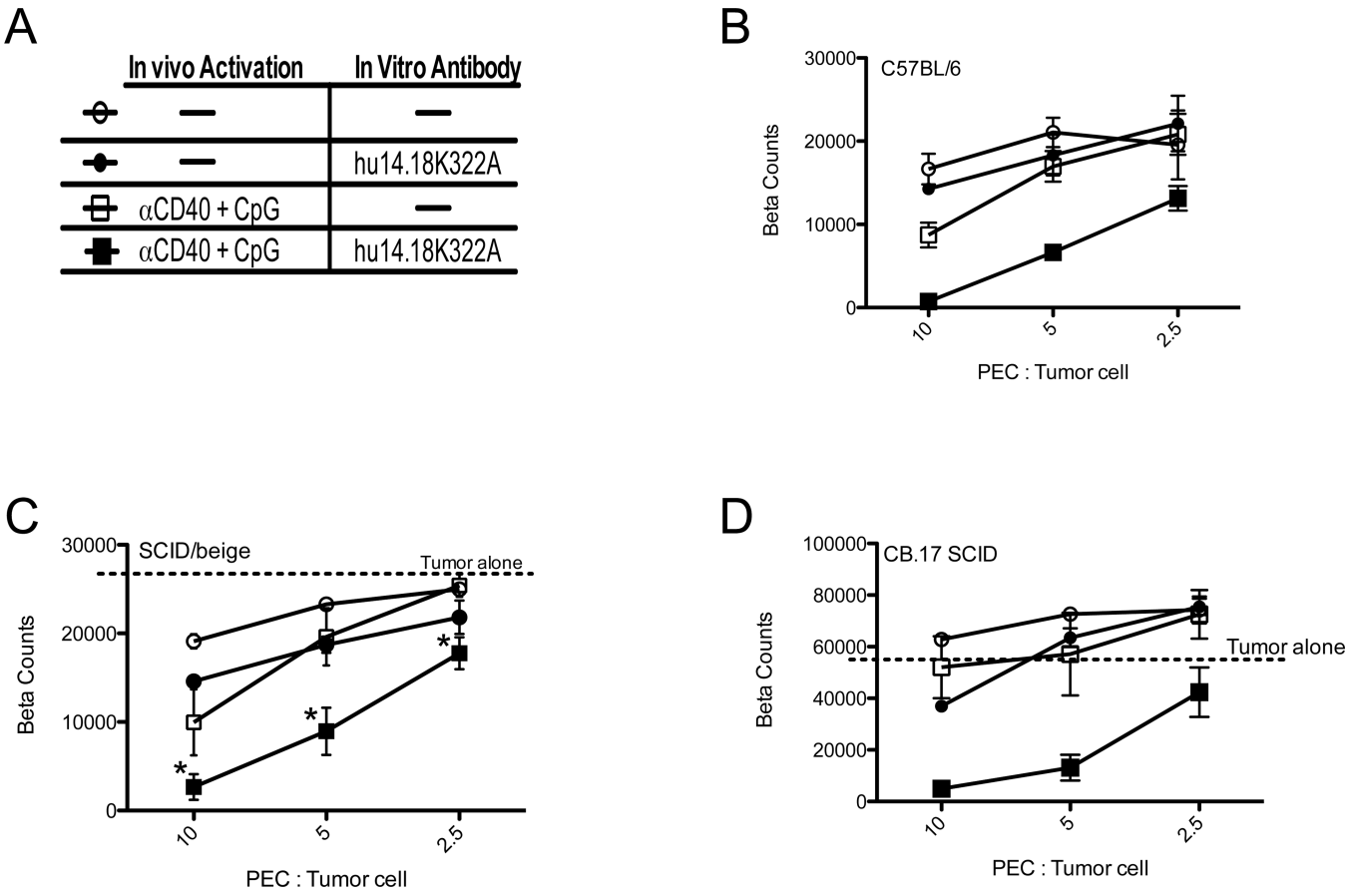

Figure 6. Activated Peritoneal Macrophages Inhibit Tumor Cells in vitro in an Antibody-dependent Manner

A) Key to labeling of symbols for data shown in Figure 6 B-D. Peritoneal cells were co-cultured with tumor cells in the presence or absence of hu14.18K322A mAb *in vitro* as described in Figure 4A. PECs were collected from either naïve mice or mice that had been pretreated with αCD40+ CpG. **B-D)** Beta counts were used to determine relative amount of tumor after co-culture (at different ratios of peritoneal cells to B78D14 tumor cells) using peritoneal cells from C57BL/6 mice (B), SCID/beige mice (C), or CB.17 SCID mice (D). *P < 0.05 comparing primed macrophages with antibody in vitro to all other conditions and determined by two-way ANOVA. C57BL/6 assay was performed four times, SCID/beige assay two times and CB.17 SCID assay one time.